communications biology

A Nature Portfolio journal

Article

https://doi.org/10.1038/s42003-025-08626-3

Ace2 mutation disrupts amino acid absorption, impairs growth, and alters microbiota dynamics in zebrafish

Kun Wu[1,3], Zhengyuan Li[1,3], Dongwei Hou[1], Taiyu Wang[1], Renjun Zhou[1], Wengen Zhu[1], Pengcheng Gao[1], Qiang Lu[1], Muhua Wang[1], Shaoping Weng[1], Wei Ge[2], Zhili He[1], Qingyun Yan[1] & Jianguo He[1] ✉

Angiotensin-converting enzyme 2 (Ace2) is a well-studied enzyme with important physiological functions in mammals. However, its roles in non-mammalian animals remain largely unexplored. This study investigates the function of Ace2 in zebrafish using CRISPR/Cas9-generated *ace2* mutants (−/−). The *ace2*$^{-/-}$ mutants exhibited significant growth retardation with reduced body length and weight. High *ace2* expression was found in the intestine, indicating its importance in gut function. Ace2 deficiency led to marked decreases in specific plasma and muscle amino acids, including cationic and neutral amino acids such as L-(+)-arginine, L-(+)-lysine, leucine, and valine, suggesting impaired amino acid absorption. The gut microbiota of *ace2*$^{-/-}$ mutants showed reduced diversity and altered bacterial communities, with marked increases in expression of genes involved in bacterial carbohydrate metabolism and marked decreases in amino acid biosynthesis pathways. These findings are consistent with enhanced carbohydrate metabolism in the liver and reduced amino acids in muscle. Our study demonstrates the essential role of Ace2 in growth, amino acid metabolism, and gut microbiota balance in zebrafish, offering novel insights into its functions across vertebrate species.

Ace2 is an enzyme with diverse biological functions beyond its classical roles in mammals[1,2]. It has been implicated in lipid metabolism, inflammation, and regulation of gut microbiota. These functions indicate that Ace2 plays important roles in various physiological and pathological processes, including metabolic disorders and immune regulation[3–6]. However, its roles in non-mammalian animals remain largely unexplored.

Recent studies have highlighted the importance of Ace2 in gastrointestinal health, including nutrient absorption, gut barrier integrity, and microbiota regulation, which are critical for maintaining metabolic and inflammatory balance[7]. Ace2 also plays a pivotal role in controlling gut dysbiosis and vascular permeability, factors associated with conditions such as diabetes and cardiovascular diseases[8,9]. Furthermore, Ace2 deficiency has been linked to impaired intestinal barrier integrity and gastrointestinal dysfunction in animal models[7,10], as well as changes in gut microbiota and intestinal health in certain pathological conditions like COVID-19.

Despite extensive research on Ace2 in mammalian systems, its roles in non-mammalian vertebrates, such as teleosts, remain largely unexplored. To assess the universality function of Ace2 across vertebrates, we conducted this study by using zebrafish as a model, which exists a homolog of Ace2. Zebrafish are widely used in biological research due to their genetic manipulability and the applicability of findings to other vertebrates[11–16]. Fish exhibit higher protein utilization and lower carbohydrate utilization, efficiently using proteins as an energy source while limiting carbohydrates[17,18]. This trait is evident in the gut microbiota, which regulates the host's energy metabolism. The gut microbiota composition in fish is closely related to protein-optimized metabolic pathways, essential for nutritional balance and energy efficiency[19,20]. Our study aims to understand the function of Ace2 and how Ace2 influences metabolic processes and intestinal function in zebrafish, providing insights into its role beyond mammalian systems.

In our study, we analyzed the spatiotemporal expression patterns of the *ace2* gene across various tissues in zebrafish. We then created a mutant zebrafish line for *ace2* using CRISPR/Cas9 technology to explore the roles of Ace2 in growth, gut microbiota, and metabolism regulation. The study findings revealed that compared to heterozygous controls (+/−), *ace2*$^{-/-}$

[1]Marine Synthetic Ecology Research Center, Guangdong Core Germplasm Bank for Marine Economic Animals, Southern Marine Science and Engineering Guangdong Laboratory (Zhuhai)/State Key Laboratory for Biocontrol, Sun Yat-sen University, 519082 Zhuhai, China. [2]Department of Biomedical Sciences and Centre of Reproduction, Development and Aging (CRDA), Faculty of Health Sciences, University of Macau, 999078 Taipa, Macau, China. [3]These authors contributed equally: Kun WU, Zhengyuan LI. ✉e-mail: lsshjg@mail.sysu.edu.cn

mutants exhibited significant growth delays, including reductions in body length and weight. Furthermore, *ace2* gene knockout significantly impacted gut microbiota diversity in the mutants, with marked reductions in the diversity indices and significant changes in the composition of the microbiota. These results suggest that Ace2 plays a crucial role in the growth and development of zebrafish and may influence the host's overall metabolic state by regulating the diversity and composition of gut microbiota. Therefore, this research sheds light on the functional roles of Ace2/*ace2* in zebrafish and offers new perspectives on its role in vertebrate physiology and the interactions among host growth, gut microbiota, and metabolism.

Results

Ace2 deficiency led to growth retardation in zebrafish

To explore the roles of Ace2 in zebrafish, we first analyzed the tissue distribution of *ace2*. The expression levels of *ace2* were relatively high in the intestine and liver compared to other tissues (Fig. 1a), suggesting its important role in gut and liver. To further verify the functionality of Ace2 in zebrafish, we generated an *ace2* null mutant fish line with CRISPR/Cas9 technology. An sgRNA targeting exon 1 of *ace2* was used to generate mutations; we selected a 7-base pair deletion [*ace2*(-7)] as it is predicted to induce frameshift mutation that disrupts Ace2 protein synthesis (Fig. 1b and Supplementary Fig. 1a). In order to determine whether this allele affected gene expression, qPCR was performed using three different primer pairs targeting separate regions of *ace2* mRNA. The results showed that *ace2* expression was clearly reduced in the mutants compared to controls (Supplementary Fig. 1b), supporting the successful knockout.

Notably, the growth of *ace2* homozygous mutants (−/−) was significantly reduced compared to the heterozygous controls (+/−) between 16-50 days post fertilization (dpf) in co-housed feeding (Supplementary Fig. 2a, b and Fig. 1c–e). No significant difference in body length was observed at 12 dpf (Supplementary Fig. 2a), but a clear reduction became detectable by 16 dpf in body length. This growth reduced in $ace2^{-/-}$ mutants were consistently observed at 20, 30, and 50 dpf (Supplementary Fig. 2a, b and Fig. 1c–e). To exclude potential growth differences caused by co-housed feeding, we raised the fish separately under identical conditions. Both body length and weight were significantly lower in $ace2^{-/-}$ mutants compared to controls at 40 dpf under separate feeding conditions (Supplementary Fig. 2c, d), indicating a clear reduction in growth rate. The above results underscored the critical role of Ace2 in growth.

Also, to investigate the molecular mechanisms underlying the growth retardation observed in Ace2 knockout zebrafish and to uncover the associated transcriptional changes, we performed transcriptomic analysis on 16 dpf larvae. The results revealed significant alterations in the transcriptomic profiles between the $ace2^{-/-}$ mutants and controls. Notably, several immune-related pathways, such as the intestinal immune network for IgA production, phagosome, and Toll-like receptor signaling pathways, were markedly downregulated (Supplementary Fig. 3). These findings suggest that the loss of *ace2* triggers widespread changes in gene expression within the zebrafish intestine.

To further assess the growth performance of $ace2^{-/-}$ mutants, we compared them with their sibling heterozygous controls at 110 dpf, the adult stage (Fig. 1f). Although both body length and body weight were significantly lower in $ace2^{-/-}$ mutants compared to the controls at 110 dpf, the difference was less pronounced than at 50 dpf (Fig. 1i). These results suggest that Ace2 disruption slowed down but does not completely block growth. We also assessed the mRNA expression levels of growth hormone (*gh*) in the pituitary. Gh, which is essential for normal physical growth, was significantly lower in $ace2^{-/-}$ mutants compared to that in the controls (Fig. 1j). The reduced expression of *gh* in $ace2^{-/-}$ mutants indicated a potential link between Ace2 and the regulation of *gh*, possibly mediated through nutritional status. The expression of *gh* is closely related to the intake and absorption of nutrients[21,22]. In summary, our results suggest that Ace2 is vital for the normal growth of zebrafish, and its effect on *gh* may be through the regulation of nutrient absorption and metabolism in intestine.

Ace2 deficiency affected the amino acids metabolism in zebrafish

The expression of amino acid transport protein B0AT1 (a sodium-dependent neutral amino acid transporter) in the intestinal tract of Ace2-deficient mice was significantly decreased. It has been previously reported that Ace2 heterodimerizes with B0AT1 in small intestinal mucosal epithelial cells to form a transport complex, thereby regulating the transport of corresponding amino acids, which revealed the role of Ace2 in the intestinal amino acid transport process of mice[23]. Also, single-cell sequencing databases from two studies have both shown that zebrafish *ace2* is specifically expressed in intestinal epithelial cells, which are the primary sites for amino acid transport and absorption in the intestine, suggesting an important role for *ace2* in the transport and absorption of amino acids in the zebrafish[24,25]. In this study, to assess the physiological consequences of Ace2 loss, we detected the content of total amino acids in $ace2^{-/-}$ mutants and their sibling controls at 110 dpf. Both plasma and muscle showed significant reductions in total amino acids in the absence of Ace2, underscoring its critical role in amino acid metabolism (Fig. 2a, b). Histological analysis revealed that muscle density was significantly lower in $ace2^{-/-}$ mutants than in controls, indicating that muscle content was lower in the in $ace2^{-/-}$ mutants than in the control (Fig. 2c, d). Furthermore, amino acid specific metabolome analysis showed that disruption of Ace2 caused significant changes in muscle amino acid metabolism (Fig. 2e–g). In zebrafish $ace2^{-/-}$ mutants, the levels of cationic amino acids, such as L-(+)-Arginine and L-(+)-Lysine, were markedly reduced, with a more than three-fold decrease compared to controls (Fig. 2h). Additionally, neutral amino acids, including L-Leucine and valine, also showed notable reductions (Fig. 2h). These results suggest that Ace2 deficiency primarily affects the transport of cationic and neutral amino acids, which are crucial for fish growth, highlighting Ace2's important role in regulating fish growth through modulation of amino acid metabolism.

Differences in bacterial composition between the mutant and control groups

Zebrafish Ace2 is primarily expressed in the intestine and liver, with the highest expression in the intestine (Fig. 1a). Growth depends on food utilization and intestinal function, with the intestine being crucial for nutrient absorption and energy acquisition[26]. The intestine also hosts microbes that regulate metabolism and support growth[27]. Therefore, we performed third-generation full-length 16S rRNA amplicon sequencing on the intestines of both zebrafish Ace2 mutants and control groups. Venn analysis results showed that there were 1,883 operational taxonomic units (OTUs) in all zebrafish guts, among which were 1,742 and 537 OTUs of the control and mutant groups, respectively (Fig. 3a). OTUs represent clusters of closely related microbial sequences, serving as a fundamental unit for assessing microbial diversity and community composition[28]. A reduction in OTU count in the mutant group suggests a loss of microbial diversity, which may have implications for gut function and host metabolism. Alpha diversity, as reflected by the Chao1 and Shannon indices, which showed microbial richness and diversity respectively, was significantly lower in $ace2^{-/-}$ mutants (268 ± 30 and 3.49 ± 0.47) compared to $ace2^{+/-}$ controls (598 ± 59 and 5.74 ± 0.85) (Fig. 3b), indicating a reduction in gut microbial diversity and potential community imbalance in the mutants. Beta-diversity, which assesses the differences in microbial community composition between groups, was analyzed using non-metric multidimensional scaling (NMDS). The results (stress = 0.085) revealed a substantial variation in the gut microbial community structures between these two groups, further supported by analysis of similarity (Anosim) (Fig. 3c). More importantly, the structure of zebrafish intestinal bacterial community in the gut of $ace2^{-/-}$ mutants (−/−) was more similar than that of controls (Fig. 3c, d). Hence, the results indicated that there was a significant reduction in the diversity of the gut microbiome in the Ace2 mutants, with significant changes in the intestinal flora. This suggests that Ace2 plays an important regulatory role in gut microbiome and may be a crucial factor affecting host growth.

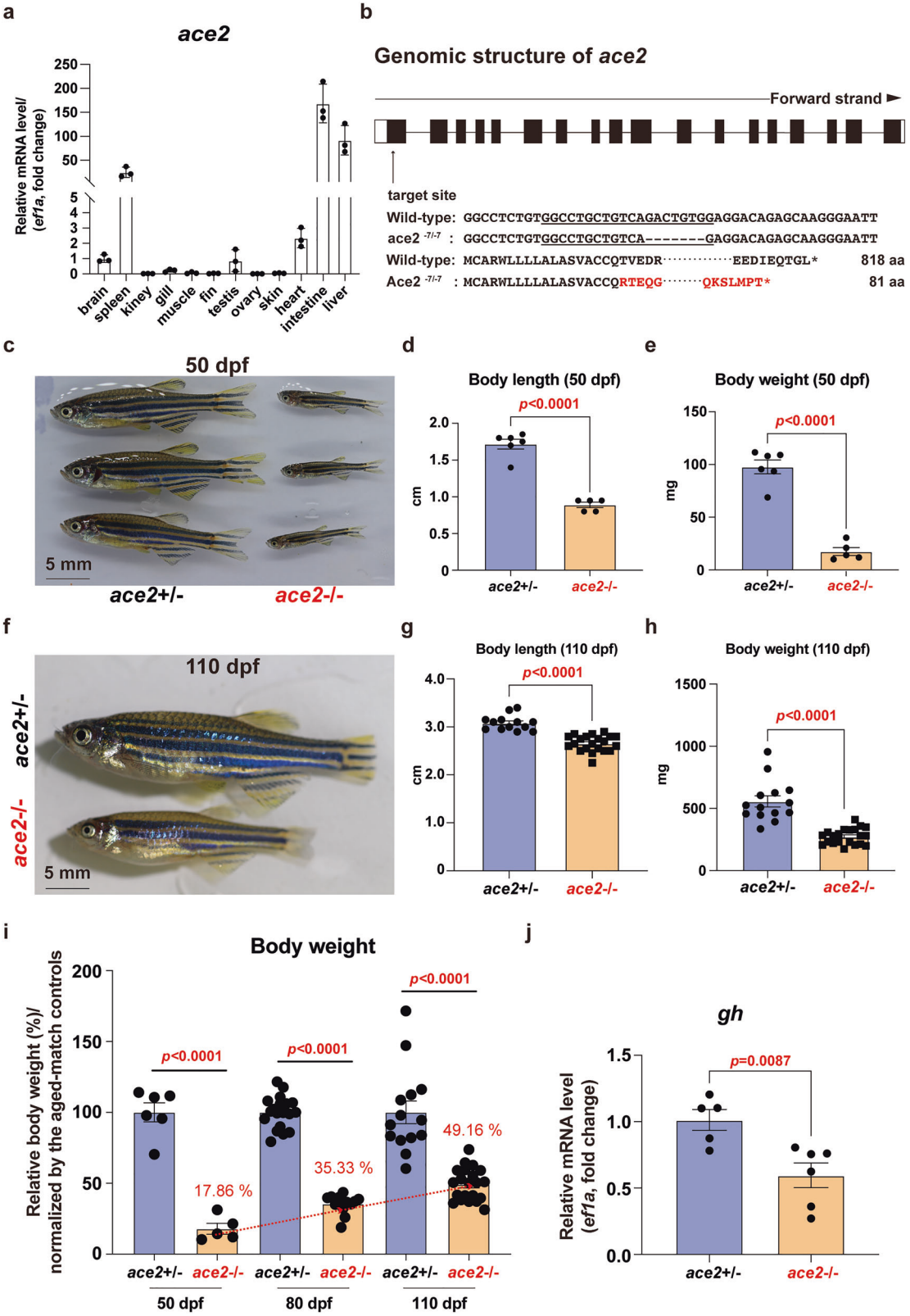

Fig. 1 | Disruption of Ace2 in zebrafish lead to growth retardation. a Quantitative real-time PCR analysis of *ace2* mRNA expression in different zebrafish tissue ($n = 3$/each group), normalized to *ef1a* as the internal control. **b** Schematic representation of the genomic structure of zebrafish *ace2* and the target site of CRISPR. Gross morphology (**c**), body length (**d**) and body weight (**e**) of zebrafish *ace2* homozygous mutants ($ace2^{-/-}$, $n = 5$) and sibling heterozygous controls ($ace2^{+/-}$, $n = 6$) at 50 dpf. Gross morphology (**f**), body length (**g**) and body weight (**h**) of zebrafish *ace2* homozygous mutants ($ace2^{-/-}$, $n = 21$) and sibling heterozygous controls ($ace2^{+/-}$, $n = 14$) at 110 dpf. **i** The relative body weight was normalized the aged-match controls at 50, 80, and 110 dpf (50 dpf: $ace2^{+/-}$, $n = 6$; $ace2^{-/-}$, $n = 5$; 80 dpf: $ace2^{+/-}$, $n = 19$; $ace2^{-/-}$, $n = 13$; 80 dpf: $ace2^{+/-}$, $n = 14$; $ace2^{-/-}$, $n = 21$). **j** The growth hormones (GH) encoded gene *gh* mRNA expression levels in zebrafish pituitary at 80 dpf assessed by quantitative real-time PCR analysis ($ace2^{+/-}$, $n = 5$; $ace2^{-/-}$, $n = 6$). The significance was analyzed by Student's t-test. (**$P < 0.01$; ***$P < 0.001$).

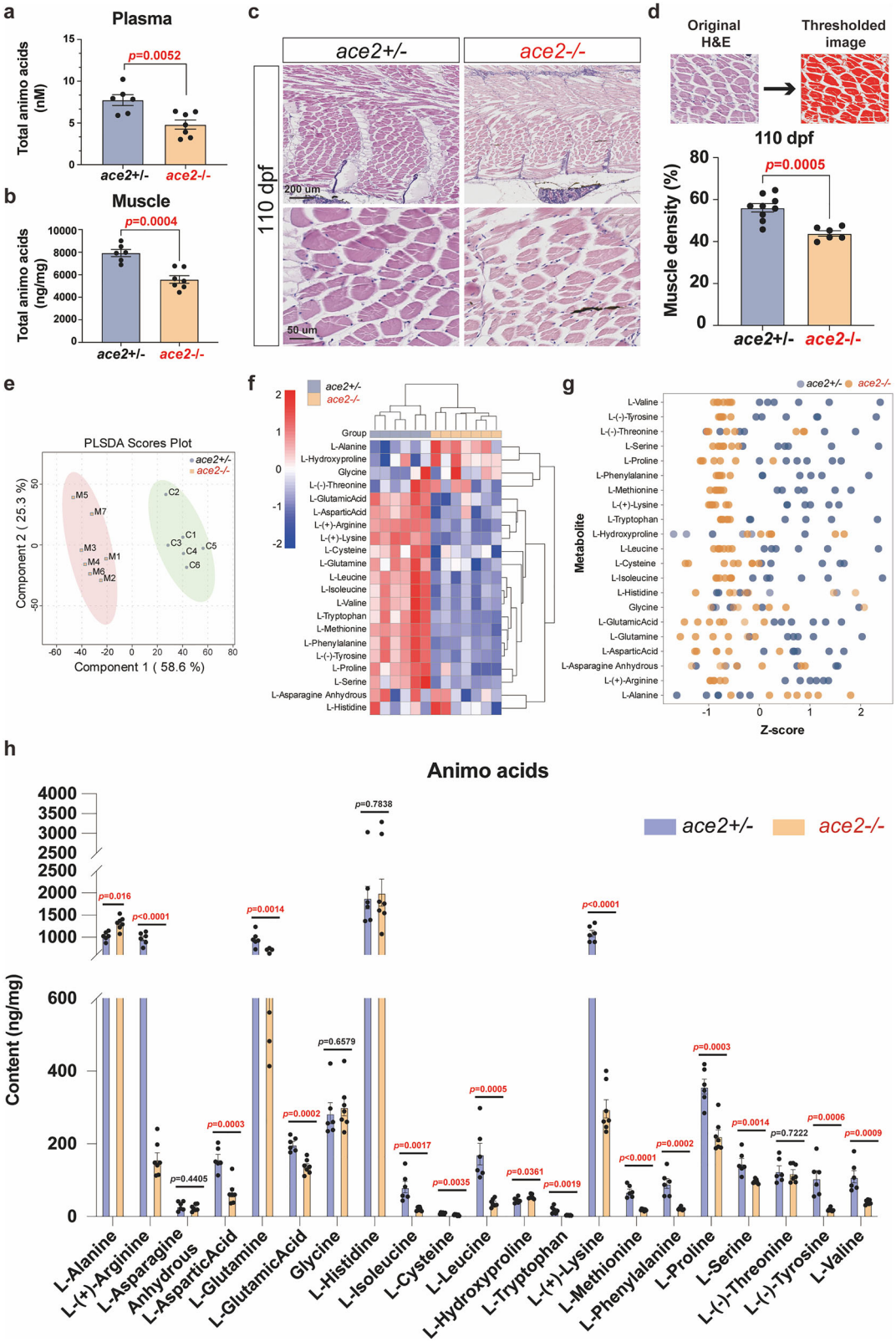

Fig. 2 | Disruption of Ace2 in zebrafish reduced the amino acids. Quantification of total amino acids in zebrafish **a** plasma and **b** muscle at 110 dpf. The significance was analyzed by Student's t-test. (**$P < 0.01$; ***$P < 0.001$; $ace2^{+/-}$, $n = 6$; $ace2^{-/-}$, $n = 7$). **c** The histological analysis in zebrafish muscle at 110 dpf. **d** The muscle density analysis in zebrafish at 110 dpf. Muscle density is calculated (software: Image J) by dividing the area of muscle fibers (the red part) in a tissue slice by the total area of the muscle. The significance was analyzed by Student's t-test. (***$P < 0.001$; $ace2^{+/-}$, $n = 6$; $ace2^{-/-}$, $n = 9$). **e** PLS-DA (Partial Least Squares Discriminant Analysis) within zebrafish muscle between the *ace2* homozygous mutants and sibling heterozygous controls at 110 dpf ($ace2^{+/-}$, $n = 6$; $ace2^{-/-}$, $n = 7$). **f** Clustering heatmap of different amino acid patterns for all samples in zebrafish muscle at 110 dpf ($ace2^{+/-}$, $n = 6$; $ace2^{-/-}$, $n = 7$). **g** The distribution of amino acid metabolites in each sample revealed by Z-score analysis ($ace2^{+/-}$, $n = 6$; $ace2^{-/-}$, $n = 7$). **h** The contents of different amino acids in zebrafish muscle at 110 dpf. The significance was analyzed by Student's t-test. (*$P < 0.05$; **$P < 0.01$; ***$P < 0.001$; $ace2^{+/-}$, $n = 6$; $ace2^{-/-}$, $n = 7$).

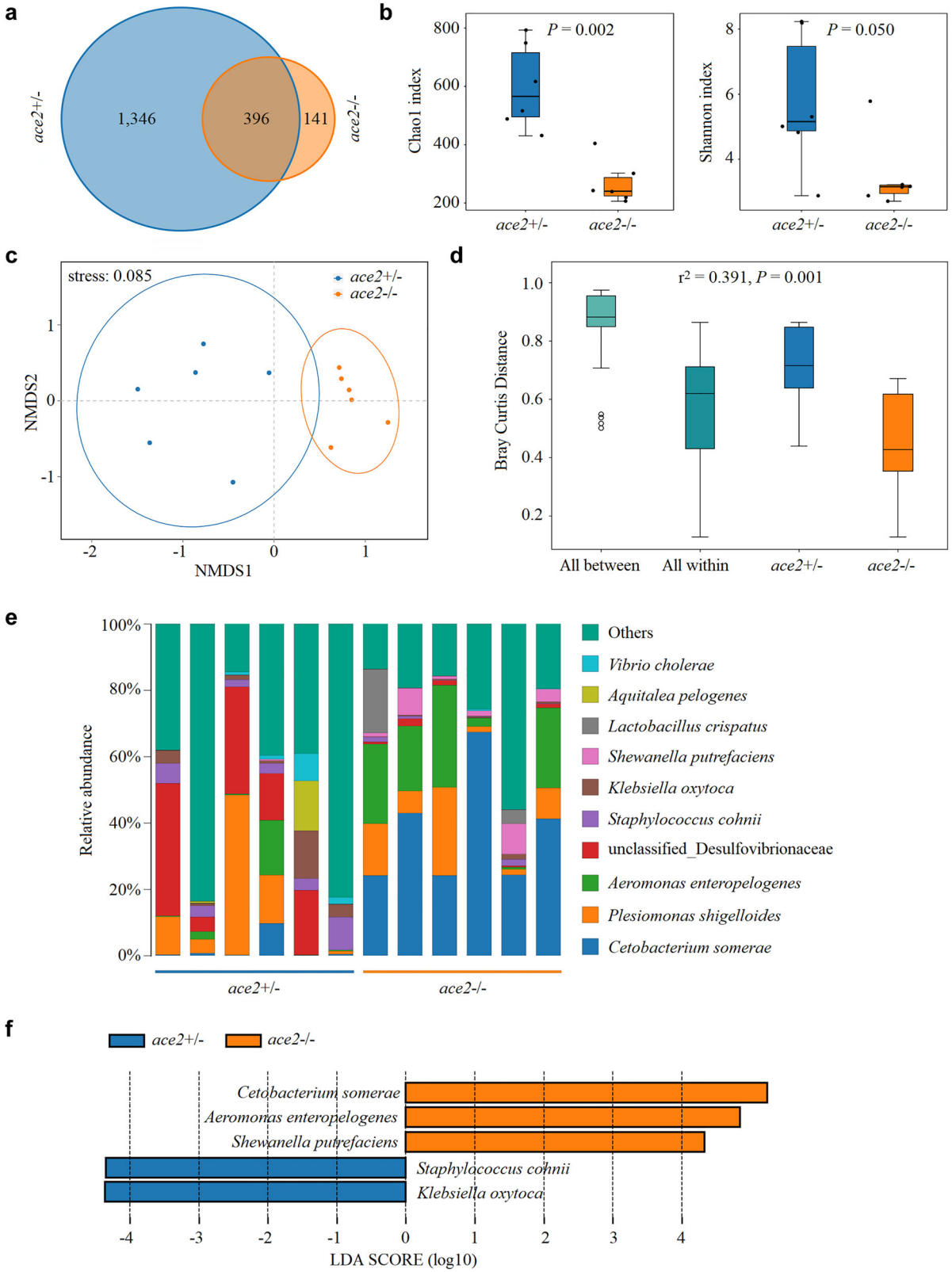

Fig. 3 | Disruption of Ace2 in zebrafish significantly decreased intestinal microbial diversity and altered intestinal community composition. a Bacterial OTU numbers in the *ace2* homozygous mutants and sibling heterozygous controls at 110 dpf, respectively ($n = 6$/each group). **b** Difference in the gut bacterial α-diversity of zebrafish between the *ace2* homozygous mutants and sibling heterozygous controls at 110 dpf ($n = 6$/each group). **c** Non-metric multidimensional scaling (NMDS) and **d** analysis of similarity (Anosim) results showed that there were significantly ($P = 0.001$) differences in gut community structure between the *ace2* homozygous mutants and sibling heterozygous controls at 110 dpf ($n = 6$/each group). **e** Differences in the bacterial community composition within zebrafish gut between the *ace2* homozygous mutants and sibling heterozygous controls at 110 dpf ($n = 6$/each group). **f** LEfSe results of bacterial indicator species in guts of the *ace2* homozygous mutants and sibling heterozygous controls at 110 dpf ($n = 6$/each group).

The bacterial composition in the gut of *ace2*$^{-/-}$ mutants exhibited significant changes compared to controls (Fig. 3e). In gut of *ace2*$^{+/-}$ controls, the ten most relatively abundant species were the unclassified *Desulfovibrionaceae*, *Staphylococcus cohnii*, *Aeromonas enteropelogenes*, *Cetobacterium somerae*, *Chryseobacterium formosense*, *alpha proteobacterium* LS96, *Sinirhodobacter hungdaonensis*, unclassified *Alphaproteobacteria*, *Corynebacterium tuberculostearicum*, and *Leuconostoc pseudomesenteroides*, which accounted for 18.36%, 4.68%, 3.29%, 1.85%, 0.71%, 0.58%, 0.52%, 0.51%, 0.48% and 0.42%, respectively. While in the gut of *ace2*$^{-/-}$ mutants, the ten most relatively abundant species were the *Cetobacterium somerae*, *Aeromonas enteropelogenes*, *Shewanella putrefaciens*, *Cetobacterium sp. ZOR0034*, unclassified *Sutterellaceae*, unclassified *Desulfovibrionaceae, Staphylococcus cohnii, Rubrobacter bracarensis*, *Rhodovulum* sp. JC2237 and *Coraliomargarita* sp.,which accounted for 37.31%, 16.96%, 4.11%, 1.54%, 1.26%, 0.99%, 0.78%, 0.61%, 0.29%, and 0.22%, respectively. Thus, knockout of Ace2 altered the distribution of dominant bacterial species in *ace2*$^{-/-}$ mutants. We further observed notable differences in the relative abundances of some bacterial species in the zebrafish gut between these two groups. Specifically, there was a significant ($P < 0.05$ in all cases) increase in the relative abundance of 12 bacterial species, such as the *Cetobacterium somerae* and *Aeromonas enteropelogenes* of *ace2*$^{-/-}$ mutants (Supplementary Data 1). Meanwhile, there was a significant ($P < 0.05$ in all cases) decrease in the relative abundance of 46 bacterial species, such as the unclassified *Desulfovibrionaceae* and *Staphylococcus cohnii* of *ace2*$^{-/-}$ mutants (Supplementary Data 1). Linear Discriminant Analysis Effect Size (LEfSe) analysis, which used to identify statistically significant biomarkers that explain differences in microbial communities, further revealed that *C. somerae*, *A. enteropelogenes* and *S. putrefaciens* were the bacterial biomarkers in the gut of *ace2*$^{-/-}$ mutants (Fig. 3f). Therefore, knockout of *ace2* exerted a stronger selective pressure on the bacterial taxa in zebrafish guts. Furthermore, knockout of *ace2* significantly changed the bacterial composition of zebrafish and so likely affects gut bacterial function.

Similar alterations were observed at earlier developmental stages. At 16 dpf, *ace2*$^{-/-}$ mutants showed reduced α-diversity and distinct microbial structures, accompanied by growth defects. At 30 dpf, although α-diversity differences were no longer significant, β-diversity remained altered, indicating persistent microbiome remodeling (Supplementary Fig. 4). Together, these results highlight the role of Ace2 in shaping gut microbial communities throughout development, with potential implications for nutrient metabolism and growth.

Differences in potential bacterial functions between the mutant and control groups

The principal component analysis (PCA) results, which was based on microbial content from 16S rRNA sequencing, indicated that the predicted functional contents of the bacterial community in zebrafish gut of *ace2*$^{-/-}$ group were clearly separated from those of control group (Fig. 4a). Several pathways were significantly ($P < 0.05$) enriched in the gut of *ace2*$^{-/-}$ group, especially the genes associated with starch and sucrose metabolism, purine metabolism, homologous recombination, pyrimidine metabolism, pentose phosphate pathway, beta-Lactam resistance, phosphotransferase system (PTS), lysine biosynthesis, amino sugar and nucleotide sugar metabolism, ribosome, quorum sensing, porphyrin and chlorophyll metabolism (Fig. 4b). In contrast, the genes associated with arginine biosynthesis, glyoxylate and dicarboxylate metabolism, "phenylalanine, tyrosine and tryptophan biosynthesis", 2-Oxocarboxylic acid metabolism, "glycine, serine and threonine metabolism", biosynthesis of amino acids, microbial metabolism in diverse environments, biosynthesis of antibiotics and oxidative phosphorylation were significantly ($P < 0.05$ in all cases) less abundant in *ace2*$^{-/-}$ group (Fig. 4b). Overall, the potential functions of the gut bacterial community were markedly different between the control and *ace2*$^{-/-}$ zebrafish. For instance, bacterial pathways involved in protein metabolism and biosynthesis were markedly decreased in *ace2*$^{-/-}$ mutants (Fig. 2), consistent with their reduced amino acid profiles while pathways related to carbohydrate metabolism showed enhanced (Fig. 4b), indicating potentially compromised energy utilization and storage in *ace2*$^{-/-}$ mutants might be changed.

We further analyzed the predicted functional composition of the gut microbiota in juvenile zebrafish (at 16 and 30 dpf). Similar to the adult stage, pathways related to protein metabolism and biosynthesis were significantly downregulated in *ace2*$^{-/-}$ mutants, likely due to impaired amino acid transport caused by Ace2 deficiency. However, unlike in adults, carbohydrate metabolism pathways did not show a marked upregulation at this stage (Supplementary Fig. 5).

Glucose metabolism was enhanced in the absence of Ace2

In the context of Ace2 deficiency, there was a noted decrease in zebrafish growth (Fig. 1), accompany by a reduction in total amino acid levels in both the blood and muscle (Fig. 2). This insufficiency in amino acid supply likely prompted a shift in metabolic pathways related to nutrient metabolism. Also, Ace2 knockout resulted in a diminished capacity for amino acid metabolism within the gut microbiota, while concurrently enhancing bacterial pathways related to starch and sucrose metabolism, indicating increased expression of genes associated with carbohydrate metabolism (Fig. 4b).

By 110 dpf, the body weight difference between Ace2 mutants and controls decreased, indicating compensatory growth (Fig. 1i). To investigate the underlying mechanism, we examined key genes in the hepatic insulin-like growth factor (IGF) signaling, a critical downstream effector of the hypothalamic-pituitary-somatotropic (HPS) axis involved in somatic growth and cell proliferation[29,30]. Our results showed elevated expressions of the *igf* signaling genes *igf1*, *igf2a*, and *igf2b* in Ace2-deficient zebrafish. Furthermore, there was significant upregulation in the expressions of *igf* receptors *igf1ra*, *igf1rb*, and *igf2r* (Fig. 5a–f), indicating activation of the IGF signaling pathway that may contribute to the compensatory growth[31].

Activation of IGF signaling and compensatory growth suggest that Ace2 mutants undergo metabolic remodeling in response to impaired amino acid metabolism. Consistent with this, elevated expression of glucose transporter (*glut2*) and glycogen synthesis-related (*ugp2a*) genes (Fig. 5g, h), along with glycolytic enzymes (*hk1*, *hk2*, *pklr*; Fig. 5i–l), might indicate a potential shift toward carbohydrate catabolism. To further substantiate this observation, we performed non-targeted metabolomic profiling of muscle in addition to the previous targeted amino acid analyses (Fig. 5m–o). PCA revealed a clear metabolic distinction between *ace2*$^{-/-}$ mutants and controls (Fig. 5m), with 155 metabolites significantly increased and 139 decreased (Fig. 5n). KEGG-based differential abundance score analysis revealed a coordinated downregulation of amino acid metabolism pathways, including arginine biosynthesis, arginine and proline metabolism, lysine degradation, D-amino acid metabolism, and glutathione metabolism. Conversely, the citrate cycle (TCA cycle), a core component of carbohydrate metabolism, was significantly increased (Fig. 5o). Together, these findings suggest that Ace2 deficiency induces metabolic reprogramming characterized by impaired amino acid metabolism and enhanced glucose utilization, which may compensate for growth retardation through IGF signaling.

Discussion

In this study, we generated an *ace2* zebrafish mutant line using CRISPR/Cas9 technology to provide compelling insights into the biological roles of Ace2 in vertebrates, particularly in fish models. The *ace2*$^{-/-}$ exhibited not only growth retardation but also significant alterations in gut microbial diversity and function, which correlated with changes in nutrient metabolism. The observed reductions in amino acids in *ace2*$^{-/-}$ mutants highlight the role of Ace2 in amino acid transport and metabolism, aligning with findings in other vertebrates and indicating a conserved function across species. Moreover, the alterations in the gut microbiota and their functional pathways suggest a link between Ace2, gut microbial, and host metabolism. These findings support the hypothesis that Ace2 is crucial for amino acid absorption and growth. Additionally, the microbial shifts in the absence of Ace2 help the fish adapt to amino acid deficiencies, providing an alternative

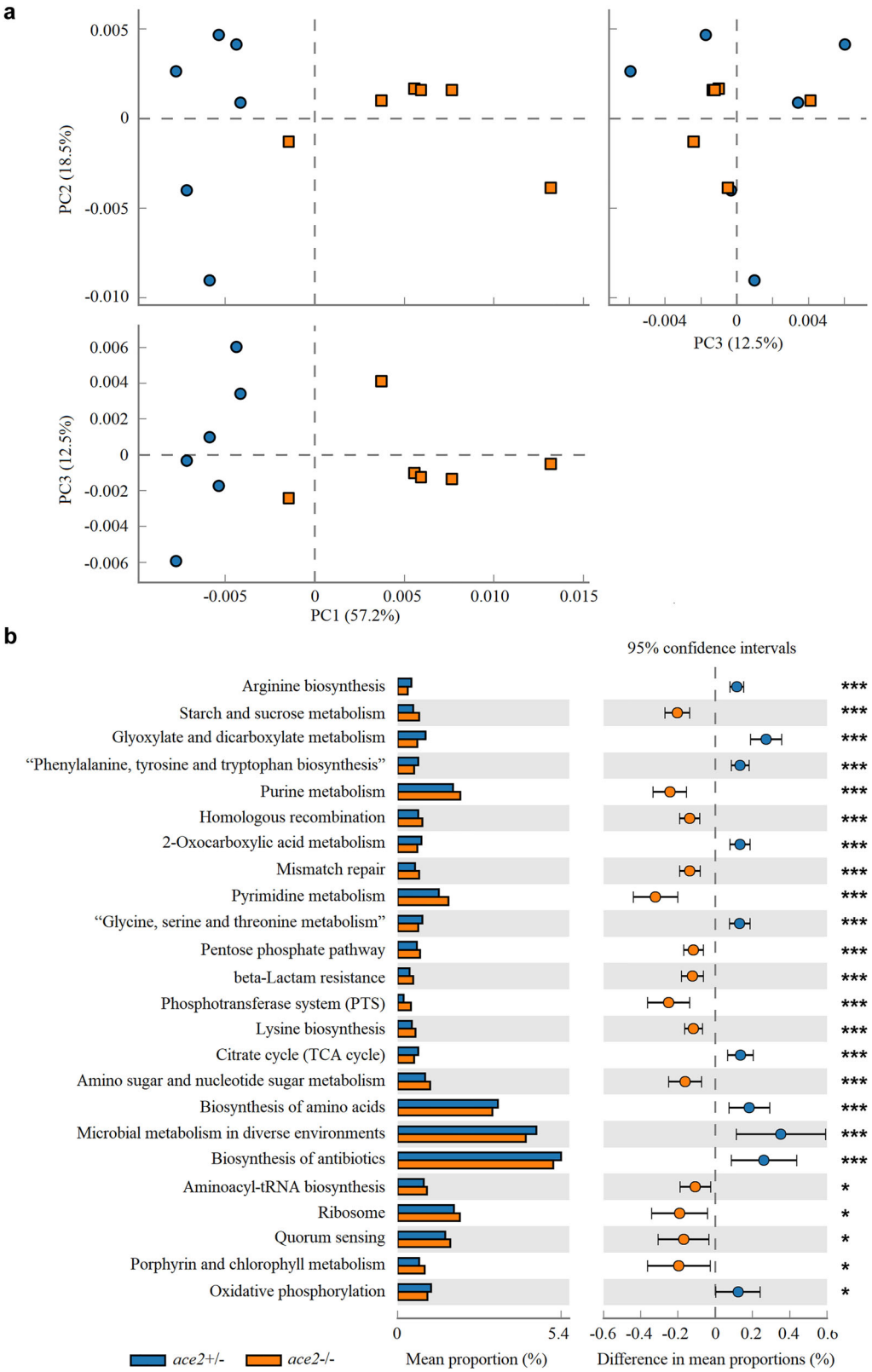

Fig. 4 | Disruption of Ace2 in zebrafish significantly altered the bacterial functional in gut. a PCA results of predicted functional content of bacterial community in zebrafish gut between the *ace2* homozygous mutants and sibling heterozygous controls at 110 dpf. **b** Predicted bacterial functional gene comparisons in zebrafish gut between these two groups. $^{*}P < 0.05$, $^{***}P < 0.001$.

metabolic strategy to support growth. This indicates that by reducing or interfering with amino acid transport, the host can enhance glucose utilization mediated by the gut microbiota, thereby regulating growth and development and partially compensating for growth demands (Fig. 6).

Ace2 is crucial for growth, as demonstrated in various studies and supported by our findings on zebrafish *ace2* mutants. Ace2 mutants ($ace2^{-/-}$) showed significant growth retardation, including reduced body length and weight compared to controls. This is consistent with the previous

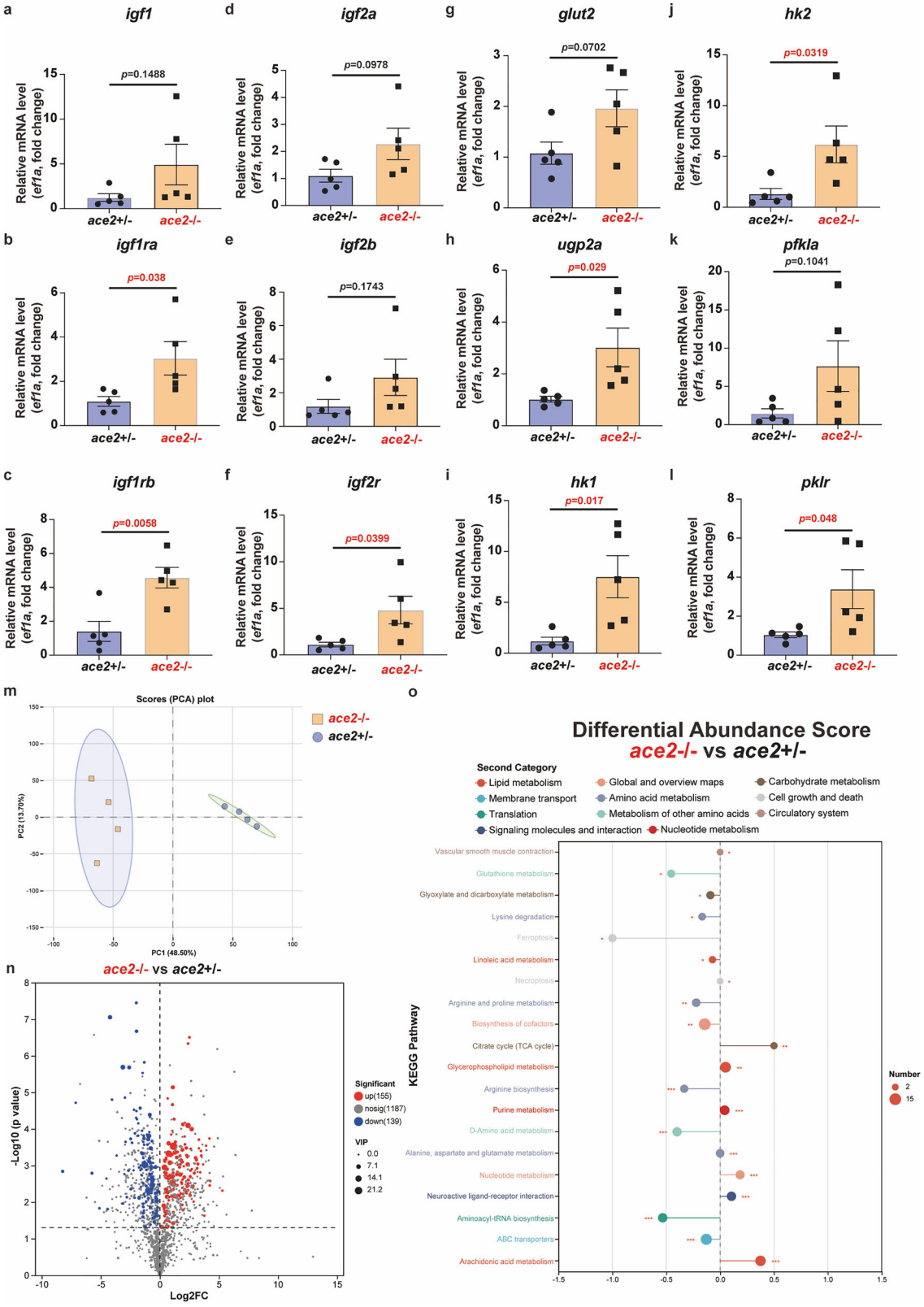

studies in mice, who reported that Ace2 deficiency impairs intestinal barrier integrity and leads to gastrointestinal dysfunction, subsequently affecting overall growth[7,10]. Ace2 knockout mice exhibited a body weight reduction of 4%-20% compared to the control group at various testing ages; however, in our study, we found that Ace2 deficiency also resulted in a severe weight decrease in zebrafish, with body weight in mutant groups being 82% and 51% lower than that of the age-matched control group at 50 and 110 dpf, respectively (Fig. 1), suggesting the significant role of Ace2 on fish growth.

Growth is the result of nutrient utilization, and the intestine plays a key role in this process as the primary site for the absorption of nutrients such as proteins, fats, carbohydrates, and vitamins[32]. The high expression of Ace2 in the intestine, as observed in our study, further underscores its role in

Fig. 5 | Gene expression levels of glucose metabolism pathways assessed by quantitative real-time PCR analysis. a–f Expression of different genes of Igf signaling in zebrafish liver between the *ace2* homozygous mutants and sibling heterozygous controls at 110 dpf. **g** Expression of glucose transporter gene *glut2* in zebrafish liver between the *ace2* homozygous mutants and sibling heterozygous controls at 110 dpf. **h** Expression of glycogen synthesis gene *ugp2a* in zebrafish liver between the *ace2* homozygous mutants and sibling heterozygous controls at 110 dpf. **i–l** Expression of glycolysis gene *hk1*, *hk2*, *pfkla* and *pklr* in zebrafish liver between the *ace2* homozygous mutants and sibling heterozygous controls at 110 dpf. Data shown are mean ± SEM, and statistical significance was analyzed by Student's t-test. (*$P < 0.05$; **$P < 0.01$; $n = 5$/each group). **m** PCA (Principal component analysis) of non-targeted metabolomics within zebrafish muscle between the *ace2* homozygous mutants and sibling heterozygous controls at 110 dpf ($ace2^{+/-}$, $n = 4$; $ace2^{-/-}$, $n = 4$). **n** Volcano plot of differential metabolites in zebrafish muscle between the *ace2* homozygous mutants and sibling heterozygous controls at 110 dpf ($ace2^{+/-}$, $n = 4$; $ace2^{-/-}$, $n = 4$). Each dot represents a metabolite. The x-axis shows the $\log_2$ fold change ($ace2^{-/-}$ vs $ace2^{+/-}$), and the y-axis indicates the $-\log_{10}$ (P-value). Red dots represent significantly increased metabolites in $ace2^{-/-}$ ($\log_2FC > 1$ and $P < 0.05$), blue dots indicate significantly decreased metabolites ($\log_2FC < -1$ and $P < 0.05$), and grey dots represent metabolites with no significant difference. **o** KEGG pathway-based Differential Abundance Score analysis of differential metabolites in zebrafish muscle between the *ace2* homozygous mutants and sibling heterozygous controls at 110 dpf (*$P < 0.05$; **$P < 0.01$; ***$P < 0.001$; $ace2^{+/-}$, $n = 4$; $ace2^{-/-}$, $n = 4$). The plot shows the distribution of significantly altered metabolites in KEGG pathways between $ace2^{-/-}$ and $ace2^{+/-}$ muscle. The x-axis represents the differential abundance score, calculated as (number of increased metabolites/ number of decreased metabolites) divided by the square root of the total number of detected metabolites in each pathway. A higher score indicates a tendency toward upregulation in the pathway, while a lower score suggests downregulation.

Fig. 6 | A working model on the role of Ace2 in zebrafish growth and metabolic remodeling. Ace2 deficiency leads to reduced amino acid absorption in the intestine, resulting in growth retardation. Ace2 deficiency also significantly alters the composition and function of the gut microbiota. The host's energy metabolism shifts from being amino acid-dominant to carbohydrate-dominant. The altered gut microbiota and the shift to carbohydrate metabolism partially compensate for the growth inhibition caused by Ace2 deficiency, even though growth differences remained significant.

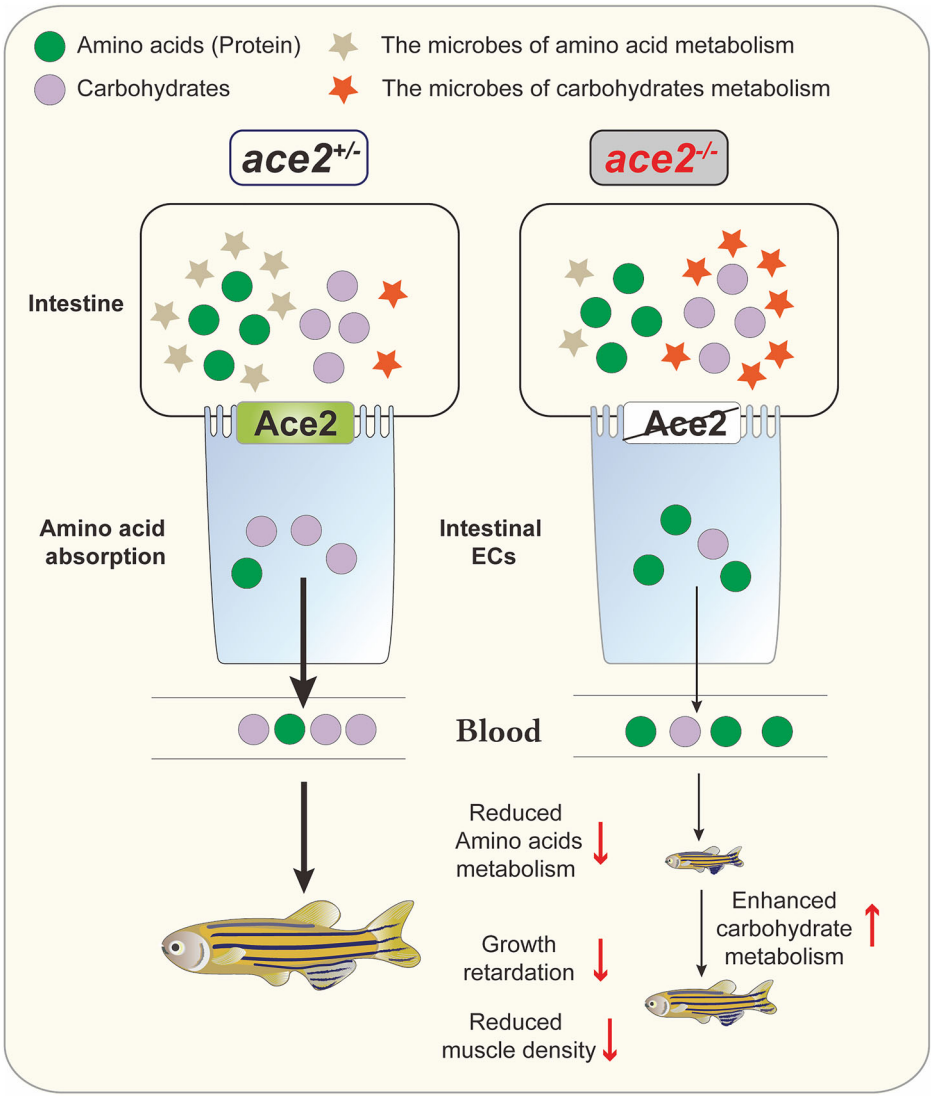

nutrient absorption for growth, which is agreed with the previous studies on Ace2 involvement in intestine function[1,4].

In Ace2-deficient mice, the transport of neutral amino acids like tryptophan is impaired due to the disruption of the Ace2-B0AT1 transport complex in the small intestine[23]. When wild-type mice and Ace2 mutant mice were fed a high-protein diet, the relative weight gain of Ace2 mutant mice was similar to that of the wild-type controls, indicating that a high-protein diet can compensate for the effects of insufficient amino acid transport due to the Ace2 mutation. However, when wild-type mice and Ace2 mutant mice were fed a low-protein diet, the wild-type mice continued to grow effectively, while the growth of Ace2 mutant mice completely stalled, indicating that under low-nutrition conditions, Ace2-mediated amino acid transport plays a major role in growth[10]. Therefore, Ace2-mediated amino acid transport is crucial for efficient protein utilization in mice, and this role is particularly important in protein depleted diets.

The growth of $ace2^{-/-}$ mutants was significantly inhibited, even under conditions of overfeeding to the point of visible satiety, indicating that the Ace2 mutation may impair nutrient absorption in zebrafish. Unlike other

animals, fish have a lower ability to utilize carbohydrates; proteins and their breakdown products, amino acids, are the primary nutrients for fish growth[26]. Therefore, sufficient protein/amino acid levels in the intestine are crucial for fish growth and development[17,33]. In zebrafish, the knockout of Ace2 significantly impacts amino acid absorption, and given the protein-dependent metabolic mode of fish, the deficiency of amino acids severely affects zebrafish growth (Fig. 2a–g).

In addition, apart from tryptophan, there is a significant downregulation of a wide range of amino acids in zebrafish muscle, including those highly related to growth such as L-(+)-Arginine, L-(+)-Lysine, L-Isoleucine, L-Leucine, and L-Methionine (Fig. 2h). A high-protein diet in fish can promote the expression of growth hormone-releasing peptide transcripts in the intestines of gilthead seabream, thereby increasing Gh levels, indicating the regulatory role of nutrients on Gh[34]. Adding arginine to the diet of silver crucian carp can activate the IGF signaling pathway, thereby promoting their growth, demonstrating the important role of arginine and IGF signaling pathway in fish growth[35].

Notably, unlike in mice where Ace2 deficiency mainly affects neutral amino acids, Ace2 knockout in zebrafish led to significant reductions not only in neutral but also in cationic amino acids such as arginine and lysine. Our results collectively suggested that *ace2* plays a broader role in amino acid metabolism in fish than in mammals. Two possible mechanisms may explain this: (1) the Ace2-B0AT1 complex in fish may have acquired a novel function in transporting cationic amino acids; (2) Ace2 may form alternative transporter complexes with other B0AT1 homologs specifically mediating cationic amino acid uptake. Further investigation is needed to elucidate the underlying mechanisms.

Research indicates that Ace1 (angiotensin-converting enzyme) plays a critical role in maintaining gut homeostasis. In zebrafish, knockout of *ace1*-a molecule in the renin-angiotensin system (RAS) with functions opposing those of *ace2*-leads to significant gut inflammation, characterized by elevated inflammatory markers and altered mucosal defense, further confirming the importance of Ace1 in gut health[36]. Additionally, the high expression levels of *ace1* and *ace2* in the gut suggest their vital roles in regulating gut physiological functions.

Recent studies, including our findings, demonstrate that knocking out either *ace1* or *ace2* significantly impacts gut function. Knockout of *ace2* primarily results in disrupted amino acid metabolism, alterations in the gut microbiota, and growth inhibition, while *ace1* knockout mainly manifests as heightened inflammatory responses and increased susceptibility to enteritis. The complex interplay between Ace1 and Ace2 in regulating gut functions warrants further investigation.

We performed transcriptome and 16S amplicon sequencing on Ace2 mutants and found that Ace2 deficiency led to a significant downregulation of immune-related pathways at 16 dpf. Since inflammatory responses are typically associated with upregulation of immune markers, this immune suppression is unlikely to result from inflammation[37,38]. Instead, it may be due to impaired growth in Ace2 mutants, which hinders the proper development of the immune system. Instead, impaired growth in Ace2 mutants may hinder proper immune system development. Given the considerable *ace2* expression in the spleen (Fig. 1a)—a tissue rich in immune cells[39]—Ace2 knockout may affect immune cell development and function. Additionally, Ace2 loss in the intestine could directly impair the local immune environment and barrier function. This systemic immune dysfunction, involving both spleen and intestine, may disrupt intestinal homeostasis, as evidenced by reduced microbial diversity, altered community structure, and increased abundance of potential pathogens (Supplementary Fig. 4c, d). These observations differ from Ace1 mutants, which primarily exhibit inflammation-driven gut abnormalities, suggesting that Ace2 plays a distinct and critical role in coordinating growth, immune maturation, and gut homeostasis.

Future studies should focus on the molecular mechanisms of Ace1 and Ace2, particularly their synergistic or antagonistic roles in gut inflammation and metabolic regulation. In our research, *ace2* knockout caused significant growth inhibition and a decrease in amino acid levels, highlighting an important role in amino acid transport and/or metabolism. However, whether *ace1* knockout results in similar nutritional deficiencies and growth issues remains unclear and merits further exploration. Unraveling the interactions between Ace1 and Ace2 in gut regulation could provide new insights into gut health research. Additionally, future work will also investigate the relevant ligand-receptor interactions and signaling mechanisms that may mediate the effects observed in Ace2 mutants, which could further elucidate the complex regulation of gut homeostasis.

Ace2 deficiency significantly influenced amino acid metabolism and consequently the composition and function of the gut microbiota. Our study demonstrated substantial reductions in total amino acid levels in both plasma and muscle of *ace2*$^{-/-}$ mutants, indicating impaired amino acid metabolism. The host nutrition absorption mode changes can lead to intestinal microbial populations[40,41]. The composition of gut microbiota in fish varies according to their dietary habits[42,43]. In our study, despite consistent daily feeding routines, the impairment of Ace2 function in mutants led to disrupted intestinal amino acid absorption, significantly altering the microbial composition in *ace2*$^{-/-}$ mutants compared to controls (Fig. 3). The reduced amino acid levels directly affected the gut microbiota, as these nutrients are crucial for microbial growth and function.

Gut is a complex ecosystem where a vast array of microorganisms coexists symbiotically with the host, jointly regulating the host metabolism and growth. Previous research has found that the diversity of gut microbiota in fish is positively correlated with their developmental stages, suggesting the critical role of gut microbiota diversity in fish growth and development[44,45]. The gut microbiota supports and promotes host growth by participating in nutrient absorption, energy acquisition, and metabolic regulation. In this study, we performed full-length 16S rRNA amplicon sequencing on the intestines of *ace2* mutant zebrafish and control groups. The results showed that the gut microbiota diversity in *ace2* mutants was significantly reduced (Fig. 3), and there were notable changes in the gut microbial community (Fig. 4), suggesting that Ace2 plays crucial roles in regulating the gut microbiota and affecting host growth.

The PCA results and pathway enrichment analysis reveal that the Ace2 mutation significantly alters the metabolic functions of the gut microbiota in zebrafish (Fig. 5). Notably, an increase in carbohydrate metabolism pathways, such as starch and sucrose metabolism, suggests a compensatory response to impaired protein metabolism due to Ace2 deficiency[10,33]. Conversely, the decrease in amino acid biosynthesis pathways and energy production cycles like the TCA cycle underscores the metabolic disruptions that hinder normal growth and physiological functions[17,32]. Additionally, reduced pathways related to host defense mechanisms suggest a potential increase in vulnerability to pathogens[7]. Also, these microbial functional changes likely arise from shifts in community composition rather than gene expression alterations within individual species. In *ace2*$^{-/-}$ mutants, diminished amino acid absorption coupled with suppressed intestinal immunity creates a nutrient environment favoring the proliferation of carbohydrate-utilizing and immune-sensitive bacteria. This suggests that microbial restructuring may be driven by selective pressures stemming from host metabolic and immune modifications. These findings highlight the critical role of Ace2 in maintaining balanced gut microbiota and overall host metabolism.

Due to technical limitations, we were unable to collect gut microbiota samples before 16 dpf, making it unclear whether dysbiosis is the cause or consequence of the growth defects observed in *ace2*$^{-/-}$ mutants. One possibility is that early loss of Ace2 disrupts mucosal immunity, thereby affecting microbiota composition. Alternatively, amino acid deficiency may trigger an energy trade-off in the host, impairing immune function and growth. These mechanisms may coexist. Future studies using early-stage sampling, germ-free models, or microbiota transplantation may help clarify their causal relationships and underlying mechanisms.

The distinct differences in bacterial community and function between the mutant and control groups suggested that the Ace2 mutation has profound effects on the gut microbiota metabolic landscape. In our study, the most significant change in the gut microbiota due to the knockout of Ace2

was the marked upregulation of *Cetobacterium somerae* (Fig. 3f). In zebrafish, a study demonstrated that the gut bacterium *Cetobacterium somerae* plays a key role in regulating fish growth. The *Cetobacterium somerae* promotes host insulin expression and glucose utilization by activating the parasympathetic nervous system through its metabolic product, acetate[19]. In Ace2 mutant zebrafish, the enrichment of carbohydrate metabolism pathways suggests a compensatory mechanism for the decrease of amino acid and protein metabolism, potentially driven by the increased presence of *Cetobacterium somerae*, reflecting an adaptation to protein-derived energy deficits[33].

Fish, which predominantly rely on proteins for energy metabolism, have a higher protein utilization rate and lower carbohydrate utilization rate compared to other vertebrates, making them particularly sensitive to disruptions in amino acid absorption[17,18]. In Ace2-deficient zebrafish, the significant reduction in amino acids severely impacts growth due to their dependence on proteins as a primary energy source. However, the gut microbiota appears to adaptively respond to this nutritional challenge. Our findings showed that the Ace2 knockout led to a reorganization of the gut microbiota, which helped the host adapt to the amino acid deficiency. This microbial shift supports an alternative metabolic strategy, enhancing glucose metabolism pathways to compensate for the reduced protein utilization, as evidenced by the upregulation of genes involved in glucose transport and glycolysis in Ace2 mutants. This adaptive response is consistent with the studies, which highlighted the gut microbiota's role in regulating host energy metabolism and nutrient absorption.

The metabolic remodeling in adaption of amino acid deficiency for growth was not only supported by gut microbiota changes but also the gene expression profile in liver. Increased expression of genes involved in glucose transport (*glut2*) and glycogen synthesis (*ugp2a*) suggests an adaptive mechanism for improved glucose storage and utilization (Fig. 5g, h). Additionally, the upregulation of glycolysis pathway genes *hk1*, *hk2*, and *pklr* highlights an increased capacity for glucose breakdown and energy production, compensating for amino acid metabolism deficiencies (Fig. 5i–l). The concurrent enhancement of glycolysis and glycogen synthesis pathways reflects an overall strengthening of glucose metabolism. This conclusion is further supported by untargeted metabolomics analysis of muscle, which revealed a reduction in amino acid metabolism and a corresponding increase in glucose metabolism.

Meanwhile, as developmental age progresses, the growth differences between *ace2*$^{-/-}$ mutants and controls decrease, indicating that this gut microbiota-driven adaptive metabolic remodeling plays a role in the growth process. However, despite this adaptation, significant growth differences remain between *ace2*$^{-/-}$ mutants and controls (Fig. 1I), indicating that enhanced glucose metabolism alone cannot fully offset the loss of amino acid metabolism.

This metabolic plasticity underscores the critical role of Ace2 in balancing amino acid and glucose metabolism for optimal growth, as amino acids are crucial for protein synthesis while glucose provides essential energy. The disruption of this balance due to Ace2 deficiency emphasizes the enzyme's importance in comprehensive nutrient metabolism. Ace2 deficiency leads to impaired amino acid absorption, causing a metabolic reshaping of the gut microbiota, which compensates by enhancing carbohydrate metabolism. However, fish have low efficiency in utilizing carbohydrates, resulting in restricted growth despite adaptive changes in gut microbiota and liver metabolism. This highlights the critical role of Ace2 in balancing amino acid and glucose metabolism to support growth.

In Ace2-deficient zebrafish, early growth is suppressed, but body weight differences decrease with age, indicating compensatory growth. This phenomenon resembles the "catch-up growth" observed under nutrient restriction or hypoxia, which typically involves activation of IGF signaling pathways[31,46]. For example, Kamei et al. reported that zebrafish embryos rely on IGF1R/Akt/Erk signaling to achieve accelerated growth following re-oxygenation[31]. Our study revealed that Ace2 deficiency impairs amino acid metabolism, and compensatory growth may depend on altered nutrient utilization. Similarly, Ace2 knockout mice exhibit a metabolic shift toward increased glucose utilization, characterized by elevated respiratory exchange ratio, reduced palmitate oxidation, and upregulated expression of glucose transporters in muscle[47], consistent with the glucose metabolic adaptations observed in our zebrafish model.

IGF-1 is downregulated during resource scarcity and upregulated upon recovery[46]. IGF-1 administration in mice fed a low-protein diet nearly restored their body weight to normal levels, indicating that exogenous IGF-1 supplementation can directly counteract growth inhibition caused by nutrient deficiency[48]. Fang et al. demonstrated that IGF-1 supplementation during starvation significantly increased gluconeogenesis, restored blood glucose levels to normal, and enhanced lipid mobilization, as evidenced by elevated plasma glycerol and free fatty acids[49]. Together, these findings support the idea that activation of the IGF signaling pathway alleviates metabolic stress and promotes compensatory growth. We propose that growth delay caused by Ace2 loss is partially compensated through IGF-dependent metabolic regulation. However, it remains unclear whether metabolic reprogramming triggers IGF signaling to drive compensatory growth or if IGF signaling induces metabolic adaptations that promote compensatory growth; this causal relationship requires further investigation.

Our study demonstrated the significant role of Ace2 in zebrafish. In conclusion, this study provides genetic evidence for the function and interaction between Ace2, gut microbiota, and metabolism in zebrafish. The key discoveries can be summarized as follows: (1) Ace2 is crucial for normal growth and development, with Ace2 knockout mutants exhibiting developmental delays and significant changes in gut microbiota diversity; (2) Ace2 regulates a broader range of amino acids in fish compared to mammals, highlighting its important role in amino acid absorption; (3) The interplay between Ace2 mediated amino acid absorption and gut microbiota is vital for metabolic and physiological process in zebrafish, underscoring the enzyme's multifaceted role in nutrient metabolism.

Materials and methods

Animal

The zebrafish were reared at 28 ± 1°C with a photoperiod of 14-h light and 10-h dark in a flow-through aquarium system (Haixing, China). The larvae were reared in nursery tanks with paramecia and artemia before transfer to the aquarium system, and the adults were fed with artemia and commercial dry food. All experiments were carried out according to the protocols approved by the Institutional Animal Care and Use Committee of Sun Yat-sen University (Approval No. SYSU-IACUC-2024-B0723). We have complied with all relevant ethical regulations for animal use.

Zebrafish mutant line generation and genotyping

The CRISPR/Cas9 technique was employed to generate the *ace2* mutant in zebrafish, following established protocols and our previous study, which is briefly descripted as follows. An sgRNA targeting exon I of *ace2* was designed using online tools (https://www.crisprscan.org) to reduce the potential off-target effects, with the oligo sequence detailed in Supplementary Table 1. The gRNA was synthesized through in vitro transcription from DraI-digested pDR274 (Addgene Plasmid #42250) using the mMACHINE T7 system, adhering to the manufacturer's guidelines. Subsequently, 4.6 nl of a mixture containing gRNA (60 ng/μl) and Cas9 protein (New England Biolabs, Ipswich, MA) was injected into one- or two-cell-stage embryos using the IM 300 Microinjector (NARISHIGE, Japan). Screening of F0 mutants was performed using high-resolution melting analysis (HRMA) and heteroduplex mobility assay (HMA), with sequencing for confirmation[50,51]. F0 founders with mosaic mutations were crossed with wild-type fish to produce heterozygous F1 (+/−) offspring. Male and female F1 siblings with the same mutation were then crossed to obtain homozygous F2 (−/−) individuals.

In addition, to minimize potential off-target effects introduced by CRISPR/Cas9 genome editing, we performed multiple generations of outcrossing and selected heterozygous carriers based on genotype rather than phenotype. As a result, the growth data analyzed in this study were collected

from later generations: data in Fig. 1 were obtained from the F5 generation, and data in Supplemental Fig. 2 were obtained from the F7 generation. This approach supports the interpretation that the observed slow growth phenotype is primarily attributable to the *ace2* mutation.

Sampling and histological examination

The entire process can be referenced from our previously published article and is summarized as follows[12,15]. Fish were collected at various time points for phenotype assessment. Following anesthetization with MS222 (Sigma, St. Louis, MO), the fish were euthanized. Each fish's gross morphology was documented with a digital camera (Canon EOS 700D). For histological examination, the fish were fixed in PFA fixative for a minimum of 24 hours. Dehydration and infiltration were conducted using the ASP6025S Automatic Vacuum Tissue Processor (Leica, Wetzlar, Germany). Samples were embedded in paraffin, and serial sections of 5 μm thickness were prepared. The sections were stained with hematoxylin and eosin (H&E) and examined using the Nikon ECLIPSE Ni-U microscope (Nikon). Images were captured with the Aperio VERSA 8 scanning system (Leica, Germany). Sibling wild-type (+/+) and/or heterozygous (+/−) fish served as controls for phenotype analysis. This entire procedure was performed as described in our previous publication.

RNA extraction and quantitative real-time PCR

The entire procedure, as detailed in our previous publication, is summarized as follows[12,15]. Total RNA was isolated from the respective tissues using TRIzol (Invitrogen, Waltham, MA) as the manufacturer's instructions. M-MLV reverse transcriptase (Invitrogen) was used for reverse transcription. Real-time PCR was carried out on the CFX384 Real-Time System (Bio-Rad) with primers listed in Table S1. Primer specificity was verified through melting curve analysis. Each PCR assay included a standard curve for quantification. Gene expression levels were normalized to *ef1a* and expressed as fold changes relative to the control group.

The 16S rRNA, transcriptome sequencings and bioinformatic analysis

The entire procedure, as detailed in our previous publication, is summarized as follows[52]. Genomic DNA from the gut contents of zebrafish was extracted using the PowerFecal DNA Isolation Kit (Mobio, Carlsbad, CA, USA). The bacterial full-length 16S rRNA gene was amplified using the 27 F and 1492 R primers, following the previously described amplification program and amplicon sequencing library construction[53]. The prepared library was sequenced on a PacBio Sequel II platform (Pacific Biosciences, Menlo Park, CA, USA) by Biomarker Technologies Co. Ltd. (Beijing, China), producing single-end reads. Raw 16S rRNA sequencing data have been deposited in the SRA database of NCBI under accession numbers PRJNA1125140. The raw sequences were processed and demultiplexed using SMRT (version 8.0) to obtain circular consensus sequencing (CCS) reads. CCS assignment for each sample was performed with Lima (version 1.7.0). Quality control using cutadapt (version 2.7) discarded CCS reads without primers and those outside the 1,200-1,650 bp range. Chimera sequences were identified and removed with the UCHIME algorithm (V8.1) as described previously, resulting in clean reads. Sequences with ≥ 97% similarity were clustered into operational taxonomic units (OTUs) using USEARCH (V10.0). Taxonomy was annotated using the RDP classifier (http://sourceforge.net/projects/rdpclassifier/), diversity analysis followed the methods described in, and the phylogenetic tree was constructed as outlined in previous studies[54]. The functional prediction of the bacterial community was conducted using Tax4Fun[55].

Estimation of ecological processes governing the bacterial community assembly in zebrafish gut

In accordance with our prior publication, we utilized a phylogenetic bin-based null model (iCAMP) to assess the predominant ecological processes influencing community assembly in the zebrafish gut across both control and mutant groups. Initially, the observed taxa were categorized into 12 distinct 'bins' based on their phylogenetic relationships. Each bin's assembly process was determined through a null model analysis incorporating beta net relatedness index (βNRI) for phylogenetic diversity and modified Raup-Crick metric (RC) for taxonomic β-diversities. For bins, percentages of homogeneous and heterogeneous selection were calculated based on pairwise comparisons with βNRI values falling below -1.96 and above +1.96, respectively. Subsequently, RC was employed to categorize remaining pairwise comparisons with $|\beta NRI| \leq 1.96$: percentages of homogenizing dispersal and dispersal limitation were derived from comparisons with RC values below -0.95 and above +0.95, while those with $|\beta NRI| \leq 1.96$ and $|RC| \leq 0.95$ indicated percentages attributed to drift. This analysis was iteratively applied across all bins, with individual process fractions weighted by the relative abundance of each bin. These results were then synthesized to estimate the relative significance of each process at the community-wide level.

Zebrafish plasma extraction and total amino acids determination

The zebrafish were raised until 110 dpf to ensure sufficient body size for blood collection. For this study, total amino acids in the plasma were assessed. Each fish was anesthetized using MS-222 (Sigma-Aldrich) prior to sacrifice. Once fully anesthetized, blood samples were collected from the heart using either a glass capillary or a 10 μl pipette tip. The collected blood was immediately transferred into tubes pre-rinsed with heparin-sodium to prevent coagulation. The samples were then centrifuged at 3000 rpm (850 g) for 30 minutes at 4 °C to separate plasma. The supernatant (plasma) was carefully collected and stored for analysis. The total amino acid concentration in the plasma was measured using the Total Amino Acid Assay Kit (Jiancheng, Nanjing, China), following the manufacturer's instructions.

UHPLC-MS/MS analysis of amino acids in muscle

Each of the 21 amino acid standards (10 mg) was dissolved in 0.1 mol/L HCl and diluted to 1 mL to obtain individual stock solutions. These were combined and serially diluted with 25 mM TCA to prepare a series of working solutions. Each working solution was then mixed in equal volume with a 400 ng/mL internal standard mixture to generate calibration standards, which were transferred into 1.5 mL EP tubes for LC-MS analysis.

Accurately weigh 20 mg of tissue, add 141 μL of water and 100 μL of 0.15% DOC (deoxycholic acid), and mix thoroughly. Then add 4 μL of an internal standard solution (100 μg/mL Lys-d4/Try-d5/Gln-d4), mix well, and ultrasonicate for 10 minutes (5 °C, 40 KHz). Add 5 μL of 10 M trichloroacetic acid (TCA), mix, and freeze the sample to precipitate proteins for 10 minutes. Centrifuge at 14,000 rcf for 10 minutes at 4°C, collect 25 μL of the supernatant, and add 375 μL of water. Vortex to mix thoroughly, and filter through a 0.2 μm PTFE membrane (Biotage, Sweden).

The LC-MS/MS analysis of the samples was conducted on an ExionLC AD system coupled with a QTRAP® 6500+ mass spectrometer (Sciex, USA) at Majorbio Bio-Pharm Technology Co. Ltd. (Shanghai, China). In summary, samples were separated using an AdvanceBio MS Spent Media column (2.1 × 50 mm, 2.7 μm) at 40°C. Metabolite separation was performed at a flow rate of 0.5 mL/min using a gradient mobile phase composed of 95% acetonitrile in water with 0.1% formic acid and 10 mM ammonium formate (solvent A) and 95% acetonitrile in water with 0.1% formic acid and 10 mM ammonium formate (solvent B), over a 6-minute run time. The gradient was as follows: 0-3 min, from 90% to 60% B; 3-4 min, maintained at 60% B; 4-4.1 min, from 60% to 90% B; 4.1-6.0 min, maintained at 90% B. Samples were kept at 4 °C during analysis.

The UHPLC system, paired with the QTRAP® 6500+ mass spectrometer equipped with an electrospray ionization (ESI) source, collected the mass spectrometric data in both positive and negative ionization modes. The operational parameters were as follows: source temperature at 550 °C; collision-activated dissociation (CAD) gas at medium pressure; Ion Source Gas 1 and Gas 2 both at 50 psi; and ion-spray voltage floating (ISVF) at +5500 V for positive mode and -4500 V for negative mode.

Untargeted metabolomics profiling of muscle

50 mg of muscle tissue was precisely weighed into a 2 mL microcentrifuge tube with a 6 mm stainless steel bead. Then, 400 µL of methanol:water (4:1, v/v) containing internal standards (e.g., L-2-chlorophenylalanine, 0.02 mg/mL) was added. Samples were homogenized at –10 °C, 50 Hz for 6 minutes, followed by ultrasonic extraction at 5 °C, 40 kHz for 30 minutes. After incubation at -20 °C for 30 minutes, the samples were centrifuged at 13,000 × g, 4 °C for 15 minutes. The supernatant was transferred to autosampler vials with inserts for LC-MS analysis. A pooled QC sample was prepared by combining 20 µL of supernatant from each sample. LC-MS analysis was performed on a UHPLC-Q Exactive HF-X system (Thermo Fisher Scientific, USA) using an ACQUITY UPLC HSS T3 column (100 × 2.1 mm, 1.8 µm; Waters, USA) at 40°C. The mobile phases were: A (95% water + 5% acetonitrile, 0.1% formic acid) and B (47.5% acetonitrile + 47.5% isopropanol + 5% water, 0.1% formic acid). Injection volume was 3 µL. Mass spectra were acquired in both positive and negative ion modes with electrospray ionization. Key parameters: spray voltage ±3500 V, capillary temp 325 °C, heater temp 425 °C, sheath gas 50 arb, aux gas 13 arb, S-lens RF 50, scan range 70–1050 m/z, resolution 60,000 (full MS) and 7,500 (MS/MS), collision energy 20, 40, and 60.

RNA-seq analysis

RNA was extracted from both control and *ace2*$^{-/-}$ larvae at 16 days post-fertilization (dpf). Total RNA was extracted using MagPure Universal RNA Kit (Magen, China). RNA purity and integrity were monitored using a NanoPhotometer spectrophotometer (Implen, USA) and Agilent 2100 (Agilent, USA), respectively. The mRNA was purified from total RNA using poly-T oligo-attached magnetic beads. Paired-end sequencing libraries were constructed using the VAHTS Universal V6 RNA-seq Library Kit for Illumina (Vazyme, China) with unique index codes and sequenced with 2×150 bp chemistry on the Illumina NovaSeq X Plus platform (Illumina, USA).

Low-quality and sequencing adapter-contaminated RNA-seq reads were filtered using fastp (v0.23.4)[56] with parameters "-n 0 -q 20".RNA-seq reads were aligned to the reference genome of *D.rerio*(GenBank: GCA_000002035.4) using HISAT2 (v2.1.0)[57]. The featureCounts(v2.0.2)[58] software was employed to enumerate the number of reads aligned to each gene. The gene abundance was calculated and normalized using FPKM (fragments per kilobase per million fragments mapped). DEGs (differentially expressed genes) between groups were determined using the Deseq2 package[59]. Differential gene expression analysis was conducted with a fold change criterion of ≥2 or ≤ 0.5, and *P*-value < 0.05 was considered significant. Subsequently, the KEGG pathways (Kyoto Encyclopedia of Genes and Genomes) were analyzed for enrichment. Raw reads are accessible at the NCBI database under BioProjectID: PRJNA1248424.

Statistics and reproducibility

Venn analysis was used to compare the OTU numbers in zebrafish gut between the Control and Mut groups. The comparison of α-diversity indices between these two groups was conducted using the Student's t-test, along with an analysis of taxonomic composition at the species level. LEfSe was used to determine the bacterial indicators in the gut of the Mut zebrafish at the species level. To assess differences in the community structure between these two groups based on the Bray Curtis distance, the NMDS and Anosim were employed. The PCA was employed to analyze the similarity of predicted function content (level 3) between these two groups, and then the Student's *t*-test was used to identify differentially functional genes.

Sample numbers in the figure legends were selected to satisfy statistical power, ensure experimental robustness, and reflect available resources. Each experimental group comprised at least three independent phenotypic replicates. All values are presented as the mean ± SEM, p values and statistical significance ($p < 0.05$) were analyzed by Student's t-test or one-way ANOVA using Prism 10 (GraphPad Prism, San Diego, CA). The significance levels are indicated in the figures by exact p values or asterisk ($^{*}p < 0.05$; $^{**}p < 0.01$; $^{***}p < 0.001$; $p > 0.05$ or ns, not significant). Sample sizes correspond to independent biological replicates, and all experiments were conducted at least twice. All individual data values plotted in the figures were contained in Supplementary Date (Supplementary Date 1).

Reporting summary

Further information on research design is available in the Nature Portfolio Reporting Summary linked to this article.

Data availability

Original data generated or analyzed during this study are included in this published article or in the data repositories listed in References. Supplementary Date contains all individual data values plotted in the figures (Supplementary Date 1), whereas Supplementary Table 1 contains all primers used in this study. Raw 16S rRNA sequencing data have been deposited in the SRA database of NCBI under accession numbers PRJNA1125140. Raw reads of RNA-seq analysis are accessible at the NCBI database under BioProjectID: PRJNA1248424. Any remaining information can be obtained from the corresponding author upon reasonable request.

Received: 12 August 2024; Accepted: 29 July 2025;
Published online: 14 August 2025

References

1. Rao, A. et al. Diverse biological functions of the renin-angiotensin system. *Med. Res. Rev.* **44**, 587–605 (2024).
2. Bhushan, S. et al. Role and interaction between ACE1, ACE2 and their related genes in cardiovascular disorders. *Curr. Probl. Cardiol.* **48**, 101162 (2023).
3. Takeshita, H., Yamamoto, K., Mogi, M., Nozato, S. & Rakugi, H. Is the anti-aging effect of ACE2 due to its role in the renin-angiotensin system?-Findings from a comparison of the aging phenotypes of ACE2-deficient, Tsukuba hypertensive, and Mas-deficient mice. *Hypertens. Res.* **46**, 1210–1220 (2023).
4. Chen, Y. Y. et al. ACE2 deficiency exacerbates obesity-related glomerulopathy through its role in regulating lipid metabolism. *Cell Death Discov.* **8**, 401 (2022).
5. Blume, C. et al. A novel ACE2 isoform is expressed in human respiratory epithelia and is upregulated in response to interferons and RNA respiratory virus infection. *Nat. Genet.* **53**, 205–214 (2021).
6. Burrell, L. M., Johnston, C. I., Tikellis, C. & Cooper, M. E. ACE2, a new regulator of the renin-angiotensin system. *Trends Endocrinol. Metab.* **15**, 166–169 (2004).
7. Hashimoto, T. et al. ACE2 links amino acid malnutrition to microbial ecology and intestinal inflammation. *Nature* **487**, 477–481 (2012).
8. Gheblawi, M. et al. Angiotensin-converting enzyme 2: SARS-CoV-2 receptor and regulator of the renin-angiotensin system: celebrating the 20th anniversary of the discovery of ACE2. *Circ. Res* **126**, 1456–1474 (2020).
9. Yu, Z. et al. Recent advance of ACE2 and microbiota dysfunction in COVID-19 pathogenesis. *Heliyon* **7**, e07548 (2021).
10. Singer, D. et al. Defective intestinal amino acid absorption in Ace2 null mice. *Am. J. Physiol. Gastrointest. Liver Physiol.* **303**, G686–G695 (2012).
11. Hwang, W. Y. et al. Efficient genome editing in zebrafish using a CRISPR-Cas system. *Nat. Biotechnol.* **31**, 227–229 (2013).
12. Wu, K. et al. Genetic evidence for differential functions of figla and nobox in zebrafish ovarian differentiation and folliculogenesis. *Commun. Biol.* **6**, 1185 (2023).
13. Xia, H. et al. Zebrafish: an efficient vertebrate model for understanding role of gut microbiota. *Mol. Med.* **28**, 161 (2022).
14. Wu, K. et al. Disrupting Amh and androgen signaling reveals their distinct roles in zebrafish gonadal differentiation and gametogenesis. *Commun. Biol.* **8**, 371 (2025).
15. Wu, K., Song, W., Zhang, Z. & Ge, W. Disruption of dmrt1 rescues the all-male phenotype of the cyp19a1a mutant in zebrafish—a novel

insight into the roles of aromatase/estrogens in gonadal differentiation and early folliculogenesis. *Development* **147**, dev182758 (2020).
16. Zhang, L. et al. Vitellogenin receptor mediates heat adaptability of oocyte development in mud crabs and zebrafish. *Nat. Commun.* **16**, 3722 (2025).
17. Oliveira-Júnior, J. C. D. et al. Effects of different ratios of crude protein and non-fibrous carbohydrates on growth, metabolism, physiology, nutrient utilization and muscle cellularity of Lophiosilurus alexandri, a carnivorous freshwater fish. *Aquaculture* **540**, 736685 (2021).
18. Wilson, R. P. Utilization of dietary carbohydrate by fish. *Aquaculture* **124**, 67–80 (1994).
19. Wang, A. et al. Intestinal Cetobacterium and acetate modify glucose homeostasis via parasympathetic activation in zebrafish. *Gut Microbes* **13**, 1–15 (2021).
20. Yao, J. et al. Effect of diet supplemented with rapeseed meal or hydrolysable tannins on the growth, nutrition, and intestinal microbiota in grass carp (Ctenopharyngodon idellus). *Front. Nutr.* **6**, 154 (2019).
21. Wong, S. C. et al. Growth and the growth hormone-insulin like growth factor 1 axis in children with chronic inflammation: current evidence, gaps in knowledge, and future directions. *Endocr. Rev.* **37**, 62–110 (2016).
22. Bhutta, Z. A. et al. Severe childhood malnutrition. *Nat. Rev. Dis. Prim.* **3**, 17067 (2017).
23. Camargo, S. M. R., Vuille-Dit-Bille, R. N., Meier, C. F. & Verrey, F. ACE2 and gut amino acid transport. *Clin. Sci.***134**, 2823–2833 (2020).
24. Jones, L. O. et al. Single-cell resolution of the adult zebrafish intestine under conventional conditions and in response to an acute Vibrio cholerae infection. *Cell Rep.* **42**, 113407 (2023).
25. Willms, R. J., Jones, L. O., Hocking, J. C. & Foley, E. A cell atlas of microbe-responsive processes in the zebrafish intestine. *Cell Rep.* **38**, 110311 (2022).
26. Debnath, S. & Saikia, S. K. Absorption of protein in teleosts: a review. *Fish. Physiol. Biochem.* **47**, 313–326 (2021).
27. Krajmalnik-Brown, R., Ilhan, Z. E., Kang, D. W. & DiBaise, J. K. Effects of gut microbes on nutrient absorption and energy regulation. *Nutr. Clin. Pr.* **27**, 201–214 (2012).
28. Blaxter, M. et al. Defining operational taxonomic units using DNA barcode data. *Philos. Trans. R. Soc. Lond. B Biol. Sci.* **360**, 1935–1943 (2005).
29. Liu, J. P., Baker, J., Perkins, A. S., Robertson, E. J. & Efstratiadis, A. Mice carrying null mutations of the genes encoding insulin-like growth factor I (Igf-1) and type 1 IGF receptor (Igf1r). *Cell* **75**, 59–72 (1993).
30. Spaventi, R., Antica, M. & Pavelić, K. Insulin and insulin-like growth factor I (IGF I) in early mouse embryogenesis. *Development* **108**, 491–495 (1990).
31. Kamei, H. et al. Role of IGF signaling in catch-up growth and accelerated temporal development in zebrafish embryos in response to oxygen availability. *Development* **138**, 777–786 (2011).
32. Canosa, L. F. & Bertucci, J. I. Nutrient regulation of somatic growth in teleost fish. The interaction between somatic growth, feeding and metabolism. *Mol. Cell Endocrinol.* **518**, 111029 (2020).
33. Kim, K. W. et al. Optimum dietary protein level and protein-to-energy ratio for growth of juvenile parrot fish, Oplegnathus fasciatus. *J. World Aquac. Soc.* **48**, 467–477 (2016).
34. Babaei, S. et al. Effect of dietary macronutrients on the expression of cholecystokinin, leptin, ghrelin and neuropeptide Y in gilthead sea bream (Sparus aurata). *Gen. Comp. Endocrinol.* **240**, 121–128 (2017).
35. Tu, Y. et al. Dietary arginine requirement for gibel carp (Carassis auratus gibelio var. CAS III) reduces with fish size from 50g to 150g associated with modulation of genes involved in TOR signaling pathway. *Aquaculture* **449**, 37–47 (2015).
36. Wei, M. et al. Ace deficiency induces intestinal inflammation in zebrafish. *Int. J. Mol. Sci.* **25**, 5598 (2024).
37. Lowery, S. A., Sariol, A. & Perlman, S. Innate immune and inflammatory responses to SARS-CoV-2: implications for COVID-19. *Cell Host Microbe* **29**, 1052–1062 (2021).
38. Medzhitov, R. The spectrum of inflammatory responses. *Science* **374**, 1070–1075 (2021).
39. Sender, R. et al. The total mass, number, and distribution of immune cells in the human body. *Proc. Natl. Acad. Sci. USA* **120**, e2308511120 (2023).
40. Jain, N. & Walker, W. A. Diet and host-microbial crosstalk in postnatal intestinal immune homeostasis. *Nat. Rev. Gastroenterol. Hepatol.* **12**, 14–25 (2015).
41. Pan, D. & Yu, Z. Intestinal microbiome of poultry and its interaction with host and diet. *Gut Microbes* **5**, 108–119 (2014).
42. Rimoldi, S., Antonini, M., Gasco, L., Moroni, F. & Terova, G. Intestinal microbial communities of rainbow trout (Oncorhynchus mykiss) may be improved by feeding a Hermetia illucens meal/low-fishmeal diet. *Fish. Physiol. Biochem.* **47**, 365–380 (2021).
43. Huang, Q. et al. Diversity of gut microbiomes in marine fishes is shaped by host-related factors. *Mol. Ecol.* **29**, 5019–5034 (2020).
44. Li, X. et al. Composition of gut microbiota in the gibel carp (Carassius auratus gibelio) varies with host development. *Micro. Ecol.* **74**, 239–249 (2017).
45. Xiao, F. et al. Host development overwhelms environmental dispersal in governing the ecological succession of zebrafish gut microbiota. *NPJ Biofilms Microbiomes* **7**, 5 (2021).
46. Sirman, A. E. et al. Compensatory growth is accompanied by changes in insulin-like growth factor 1 but not markers of cellular aging in a long-lived seabird. *Am. Nat.* **202**, 78–91 (2023).
47. Bernardi, S. et al. ACE2 deficiency shifts energy metabolism towards glucose utilization. *Metab. Clin. Exp.* **64**, 406–415 (2015).
48. Nishi, H. et al. Essential amino acid intake is required for sustaining serum insulin-like growth factor-I levels but is not necessarily needed for body growth. *Cells* **11**, 1523 (2022).
49. Fang, F., Goldstein, J. L., Shi, X., Liang, G. & Brown, M. S. Unexpected role for IGF-1 in starvation: maintenance of blood glucose. *Proc. Natl. Acad. Sci. USA* **119**, e2208855119 (2022).
50. Dahlem, T. J. et al. Simple methods for generating and detecting locus-specific mutations induced with TALENs in the zebrafish genome. *PLoS Genet.* **8**, e1002861 (2012).
51. Ota, S. et al. Efficient identification of TALEN-mediated genome modifications using heteroduplex mobility assays. *Genes Cells* **18**, 450–458 (2013).
52. Hou, D., Li, H., Wang, S., Weng, S. & He, J. Nitrite nitrogen stress disrupts the intestine bacterial community by altering host-community interactions in shrimp. *Sci. Total Environ.* **925**, 171536 (2024).
53. Wang, Z. et al. Fermented soybean meal replacement in the diet of lactating holstein dairy cows: modulated rumen fermentation and ruminal microflora. *Front. Microbiol.* **12**, 625857 (2021).
54. Huson, D. H., Auch, A. F., Qi, J. & Schuster, S. C. MEGAN analysis of metagenomic data. *Genome Res.* **17**, 377–386 (2007).
55. Asshauer, K. P., Wemheuer, B., Daniel, R. & Meinicke, P. Tax4Fun: predicting functional profiles from metagenomic 16S rRNA data. *Bioinformatics* **31**, 2882–2884 (2015).
56. Chen, S., Zhou, Y., Chen, Y. & Gu, J. fastp: an ultra-fast all-in-one FASTQ preprocessor. *Bioinformatics* **34**, i884-i890 (2018).
57. Kim, D., Paggi, J. M., Park, C., Bennett, C. & Salzberg, S. L. Graph-based genome alignment and genotyping with HISAT2 and HISAT-genotype. *Nat. Biotechnol.* **37**, 907–915 (2019).
58. Liao, Y., Smyth, G. K. & Shi, W. featureCounts: an efficient general purpose program for assigning sequence reads to genomic features. *Bioinformatics* **30**, 923–930 (2014).
59. Love, M. I., Huber, W. & Anders, S. Moderated estimation of fold change and dispersion for RNA-seq data with DESeq2. *Genome Biol.* **15**, 1–21 (2014).

Acknowledgements
This study was supported by National Natural Science Foundation of China (32473128), Southern Marine Science and Engineering Guangdong Laboratory (Zhuhai) (SML2024SP001, SML2024SP002, SML2024SP022, 221425007), Guangdong Basic and Applied Basic Research Foundation (2022A1515110089), Zhuhai Social Development Science and Technology Program (2420004000181) and Guangdong S&T Programme (No. 2024B1212060001).

Author contributions
J.H. developed the hypothesis and designed the experiments. J.H. supervised and administered the project. J.H. and K.W. acquired the funding. K.W. and Z.L. performed most of the experiments, data analysis and figure production. D.H., R.Z., W.Z., M.W., Z.H. and Q.Y. performed the microbiome analysis. T.W., P.G. and Q.L sampled the zebrafish. K.W. and Z.L. drafted the original manuscript. J.H., W.G., Q.Y., Z.H. and S.W. provided critical revisions and approved the final version of the manuscript for submission. All authors contributed and approved the final manuscript.

Competing interests
The authors declare no competing interests.

Additional information
Supplementary information The online version contains supplementary material available at https://doi.org/10.1038/s42003-025-08626-3.

Correspondence and requests for materials should be addressed to Jianguo He.

Peer review information *Communications Biology* thanks Patrick Page-McCaw and the other, anonymous, reviewer for their contribution to the peer review of this work. Primary Handling Editor: Christina Karlsson Rosenthal.